Wing Leading-Edge Droop/Slot Modification for Stall Departure Resistance

H. M. Ross* and L. P. Yip†
NASA Langley Research Center, Hampton, Virginia 23665
and
J. N. Perkins,‡ R. J. Vess,§ and D. B. Owens¶
North Carolina State University, Raleigh, North Carolina 27695

Wind-tunnel and full-scale flight tests were performed on a general aviation configuration to investigate its high angle-of-attack aerodynamic characteristics. The tests were aimed at finding a wing leading-edge modification that would improve the stall departure characteristics. Test results indicated that a wing leading-edge modification was developed that greatly improved the stall characteristics of the configuration. This modification employed the use of an outboard wing leading-edge droop plus two chordwise leading-edge slots. On the wind-tunnel model, this modification was shown to produce almost no wing rock tendency when tested on a free-to-roll apparatus. When tested on the full-scale aircraft, the modification provided a gentle, very controllable stall with little or no penalty in cruise or climb performance. Lateral control of the aircraft was effective throughout the entire stall maneuver, which was performed with full elevator deflection. In general, the flight tests showed good agreement with the wind-tunnel results.

Nomenclature

b = wing span, ft
C_L = lift coefficient
C_l = rolling moment coefficient
C_{l_β} = rolling moment due to sideslip, per deg
C_m = pitching moment coefficient
C_{n_β} = yawing moment due to sideslip, per deg
S = wing area, ft^2
α = angle of attack, deg
β = angle of sideslip, deg

Introduction

WIND-TUNNEL tests and full-scale flight tests were performed on a general aviation configuration having a high aspect ratio wing (Fig. 1). Tests were performed to investigate a wing leading-edge modification for enhancing the configuration's stall departure resistance.

The wing studied had an aspect ratio of 10.4, whereas most general aviation aircraft wings have an aspect ratio of 6 to 8. One benefit of a high aspect ratio wing is the greater lift-to-drag ratio, which gives better cruise and climb performance. However, research has shown that high aspect ratio wings have multiple stall cells along the span that more conventional, lower aspect ratio wings do not have.[1] Since this configuration had a high aspect ratio wing, multiple stall cells were expected to produce undesirable characteristics in the stall regime. The airfoil sections used for the wing were a NACA 23017 at the root and a NACA 23010 at the tip. The 23000 series airfoils have been used for many general aviation aircraft due to their low pitching moment coefficients; however, these airfoils are known to have abrupt stall characteristics.[2]

One method that has recently been investigted to improve stall characteristics is the use of outboard leading-edge droops.[3-12] In most cases, leading-edge droops do not decrease maximum lift and often increase it. Leading-edge droops typically keep the outboard wing flow attached at angles of attack significantly above the basic wing stall angle of attack. The intent of providing attached flow to the outer wing panel is to provide increased roll damping and roll control near the stall. Past studies using leading-edge droops have included wind-tunnel testing, radio-controlled model flight testing, and full-scale flight testing.[5-12] Reference 9 gives the results of wind-tunnel testing performed on an airplane with a wing aspect ratio of 10.95. Flow visualization showed stall cell formation approximately halfway between the fuselage and wingtip, which is typical for high aspect ratio wings. The use of a vortex generator or a small droop segment over the stall cell in addition to an outboard droop was found to significantly enhance the configuration's roll damping characteristics at high angles of attack.

Because of aesthetic considerations and possible increase in drag at cruise, the segmented droop configuration was not

Presented as Paper 89-2237 at the AIAA 7th Applied Aerodynamics Conference, Seattle, WA, July 31–Aug. 2, 1989; received Aug. 24, 1989; revision received Oct. 8, 1990; accepted for publication Oct. 25, 1990.

*Research Engineer, Flight Dynamics Branch, Flight Applications Division, MS 355. Member AIAA.
†Research Engineer, Flight Research Branch, Flight Applications Division, MS 247. Senior Member AIAA.
‡Professor, Mechanical and Aerospace Engineering, Box 7910. Associate Fellow AIAA.
§Lecturer, Mechanical and Aerospace Engineering, Box 7910. Member AIAA.
¶Graduate Student, Doctoral Program, Box 7910. Member AIAA.

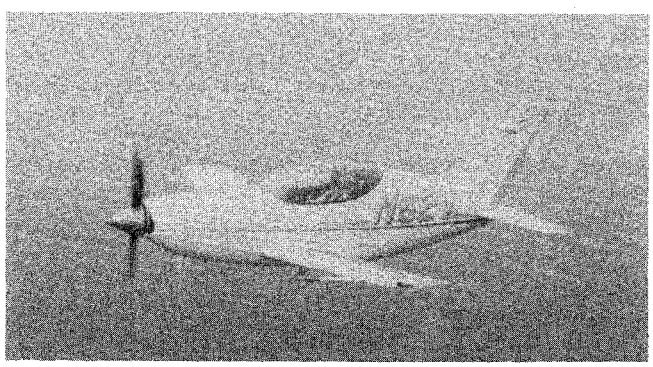

Fig. 1 Full-scale aircraft in flight.

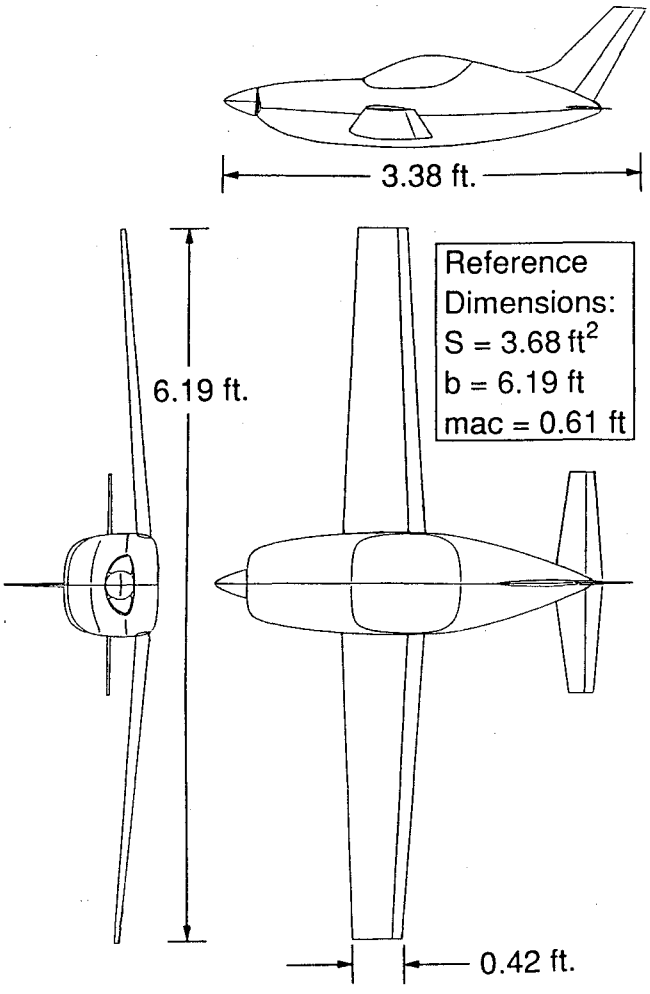

Fig. 2 Three-view sketch of the wind-tunnel model.

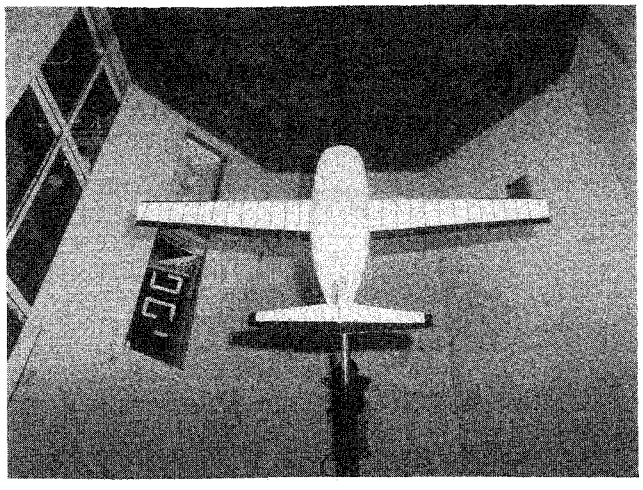

Fig. 3 Wind-tunnel model mounted in the NASA Langley 12-Foot Low-Speed Tunnel.

considered for application on this particular configuration. Another promising concept for improving wing stall characteristics was the use of chordwise leading-edge slots. The narrow slots allowed bleed air onto the wing's upper surface at high angles of attack, which created a pair of vortices that enhanced flow characteristics at high angles of attack. A slot placed near the mid semispan stall cell can re-energize the boundary layer in that area and prevent the stall cell from spreading. If a slot is used in combination with an outboard droop, the droop's effectiveness could be enhanced so that the droop could be made smaller, giving less cruise performance penalty.

It was the purpose of this investigation to find a leading-edge modification that consisted of leading-edge droops, slots, or a combination of the two that would soften the stall break and greatly increase the roll damping characteristics at stall wtihout significant loss of lift or increase in drag. Exploratory wind-tunnel testing was conducted at the NASA Langley 12-Foot Low-Speed Tunnel to investigate various configuration modifications. The leading-edge modification that appeared to be most promising from the wind-tunnel study was implemented on the full-scale aircraft for flight test evaluation. The full-scale flight testing was performed at Piedmont Triad International Airport, Greensboro, North Carolina. This paper describes the results of the investigation.

Model Description and Test Procedures

Wind-Tunnel Test

A 22.5% scale model was used for the wind-tunnel tests. The basic configuration is depicted in a three-view diagram in Fig. 2 and is shown mounted in the wind tunnel in Fig. 3. This configuration employed a full-span flaperon control surface, which deflected as flaps plus ailerons. The flaperon settings tested on the wind-tunnel model included pure flap deflections of 5, 10, and 15 deg with additional and combined aileron deflections of ± 5 and ± 10 deg. The rudder deflections ranged from 25 deg right to 25 deg left. The elevator deflections ranged from $+10$ deg (down) to -30 deg (up).

The wing modifications tested were leading-edge droops and leading-edge slots (Fig. 4). An optimization technique using a two-dimensional computer code was used to design the droop profiles. At the wingtip, the droop had an extension of 2.57% local chord and a droop of 0.77% local chord, and at the inboard edge of the droop, there was an extension of 2.44% local chord and a droop of 1.62% local chord. Shown in Fig. 5 are the droop and slot profiles. The leading-edge slots tested were 1/16 in. wide; they were 5% of the mean aerodynamic chord length deep and were cut so that the front face of the slot was vertical and flat (Fig. 5). The exact length and placement of the droop as well as the number and position of the slots were determined in the wind-tunnel tests.

Wind-tunnel testing was conducted in the NASA Langley 12-Foot Low-Speed Tunnel. These tests were done at a free-stream dynamic pressure of 4 psf with a corresponding Reynolds number of 2.26×10^5 based on the mean aerodynamic chord of the wing. Small Mylar tufts were attached to the upper surface of the wing to study regions of separated flow. The flow visualization led to stall maps that show the development and progression of stall cells. A free-to-roll apparatus was first used to evaluate various droop and slot leading-edge modifications. This type of apparatus allows the model to move freely only about the roll axis. Even though no quantitative data were taken, this testing qualitatively indicated which configuration provided the greatest amount of damping in roll. The amount of roll damping provided by the droops was judged by the amount of wing rock that they allowed. The least wing rock occurrence indicated the most damping power and, thus, the best modification.

A systematic approach was used to find the leading-edge modification that provided the best roll damping characteristics. First, the outboard droop span location was determined from tests on the free-to-roll apparatus without leading-edge slots. Spanwise cuts from the inboard edge of the droop were made in an attempt to minimize the droop span. The droop span was varied from 52.5% $b/2$ to 25.6% $b/2$ as measured from the wingtip (Fig. 6). Leading-edge slots were then tested without leading-edge droops. Sixteen slots were cut into the wing, the first being 2.7% $b/2$ from the tip with subsequent inboard slots 5.4% $b/2$ apart. The slots were numbered from 1 to 16 starting with 1 being the slot nearest the tip and 16 nearest the fuselage (Fig. 7). The number and position of

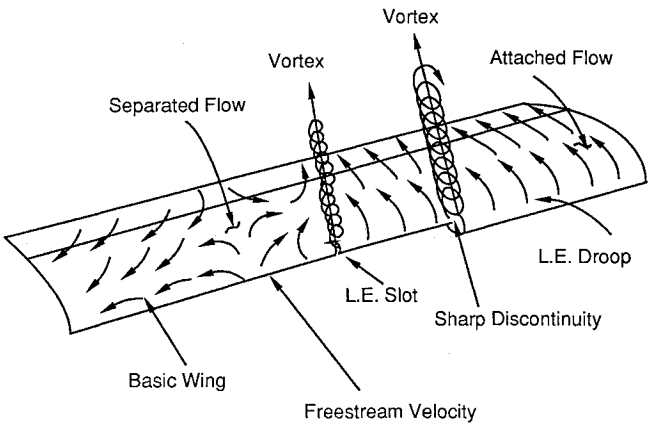

Fig. 4 Leading-edge droop and slot aerodynamics.

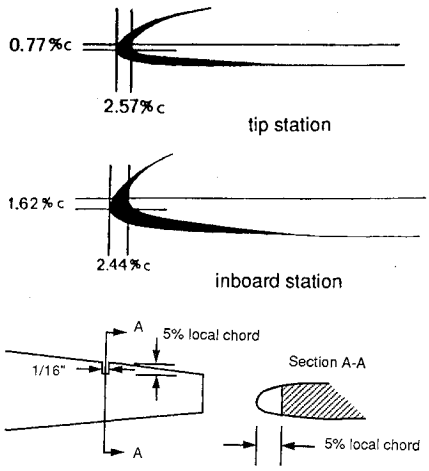

Fig. 5 Leading-edge droop and slot profiles.

leading-edge slots to provide good roll damping were determined. The results of the droop-only and slot-only testing were combined, and several droop/slot combinations were tested on the free-to-roll apparatus. When this phase of testing was complete, the model was equipped with a six-component, internally mounted strain gauge balance. Static forces and moments were measured through an angle-of-attack range of -8 to 40 deg and sideslip angles of -4, 0, and $+4$ deg for the basic configuration and the leading-edge modifications that appeared to provide the best roll damping characteristics on the free-to-roll apparatus.

Full-Scale Flight Tests

Full-scale flight tests were performed at Piedmont Triad International Airport, Greensboro, North Carolina. Tests were performed at a Reynolds number of 5.16×10^6 at the cruise velocity and 1.68×10^6 at an average stall velocity, both based on the wing mean aerodynamic chord. The full-scale aircraft had a maximum flap deflection of $+16$ deg (down), and the maximum aileron deflection was ± 8 deg (down and up) from the flap position. This translated to a maximum flaperon deflection of $+24$ deg (down) and -8 deg (up).

During stall testing, small yarn tufts were attached to the upper surface of the wing to determine the separated flow areas. The aircraft was not equipped to record flight data and so this testing was purely qualitative. Video tapes and still photographs were made for later analysis. The leading-edge droops used were constructed using templates to determine accurately the correct profile shapes at different stations, and foam was used in between the templates and shaped to the proper contour. A polyester resin was applied on top of the foam in order to make the surface smooth. The slots were cut directly into the leading edge of the wing and reinforced locally to restore structural integrity to the wing. The modified aircraft was flight tested with a center-of-gravity range from approximately 10 to 30% of the mean aerodynamic chord.

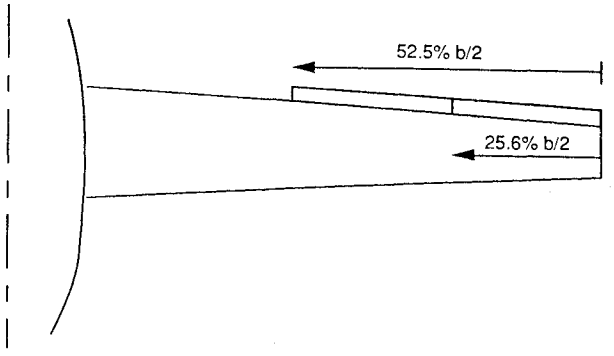

Fig. 6 Upper and lower limits of droop spans tested.

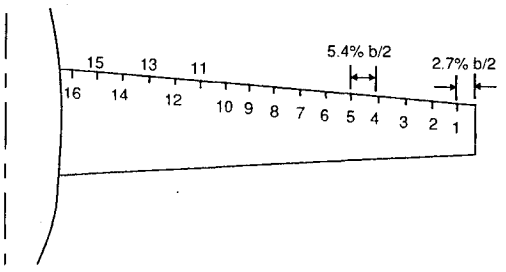

Fig. 7 Locations of leading-edge slots tested.

The leading-edge modifications that were flight tested corresponded to the optimum configuration found in the wind-tunnel study. The same leading-edge droop contour, scaled length, and spanwise position were used as determined by the wind-tunnel tests. The leading-edge slots used were 3/32 in. wide. The inboard slot depth used in full-scale testing was 1¼ in., and the outboard slot depth used in full-scale testing was 1⅛ in. The slots were less wide and deep than the scaled values would have dictated, due to the effect of Reynolds number on slot flow, but their spanwise positions were not varied with respect to the wind-tunnel model.

The types of stalls performed included power-on and power-off stalls entered from a wings level attitude and from turning flight. These stalls were performed in both a clean wing configuration and with flaps and landing gear extended, which represented the takeoff and landing configurations. The test pilot started the stall maneuvers by setting the power and then gradually decreasing the velocity by increasing the pitch attitude until the elevator was fully deflected. Power-off stalls were performed at idle power, and for the power-on stalls, the power was set from 15 to 20 in. of manifold pressure, about 35 to 48% of the maximum power. Accelerated stalls were entered similarly except that a banking turn of approximately 30 deg was started after the power was set. The pilot then deflected the elevator in climbing flight until the full deflection was achieved.

Discussion of Results

Wind-Tunnel Test

Free-to-Roll and Tuft Flow Visualization Results

Basic configuration. The free-to-roll tests showed that the baseline configuration had large amplitude roll oscillations that started at $\alpha = 16$ deg due to the loss of attached flow as seen by the tuft flow visualization. Flow visualization was achieved by attaching small Mylar tufts to the upper surface of the wing. Mylar tufts were used because they are much thinner

than conventional yarn tufts and, thus, caused less disturbance of the flow. From the tuft flow visualization, a stall map was produced showing the baseline stall pattern of the wing (Fig. 8). As expected, separation first occurred at the wingtips and wing-fuselage juncture. At $\alpha = 15$ deg, a mid semispan stall cell developed, characteristic of a high aspect ratio wing, and at that point, a large portion of the wing had separated flow. By $\alpha = 16$ deg, the inboard two-thirds of the wing had stalled, and by $\alpha = 18$ deg, the wing was completely stalled, having no attached flow on the upper surface.

Leading-edge modifications. The leading-edge modifications that were tested in order to improve the model's high angle-of-attack characteristics were leading-edge droops and leading-edge chordwise slots whose effectiveness was judged by the magnitude of wing rock and the angle of attack at which the wing rock occurred. Testing of outboard droops alone yielded the result that a single droop of 31.0% $b/2$ span delayed wing rock to approximately 20-deg angle of attack. When the chordwise leading-edge slots were tested alone, the free-to-roll results showed that 11 slots had to be open to provide good roll damping. This was realistically considered to be unacceptable. Combinations of an outboard droop with leading-edge slots were also tested on the free-to-roll apparatus. A droop of 29.6% $b/2$ span was tested with various slots open. The results showed that this droop with slots 6 and 10 open, as shown in Fig. 9, provided enough roll damping so that no wing rock occurred through the angle-of-attack range tested. The airfoil coordinates for this droop modification are given in Tables 1 and 2 at the tip and inboard stations, respectively.

Figure 10 shows the stall pattern observed by tuft flow visualization for the leading-edge modifications shown in Fig. 9. The results show that the inboard slot 10 prevented the mid semispan stall cell from developing and prevented the inboard stall from progressing to the outboard wing. Slot 6, the outboard slot, enhanced the droop edge discontinuity. At $\alpha = 18$ deg, a large portion of the outboard panel as well as the midpanel area had attached flow, whereas the baseline wing had no attached flow. This attached flow near the tip provided the roll damping observed in the free-to-roll testing and made added lateral control possible.

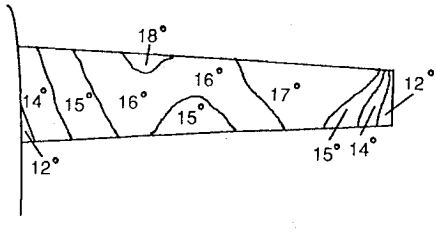

Fig. 8 Basic wing stall pattern (contour lines indicate areas of separated flow at the angle of attack shown).

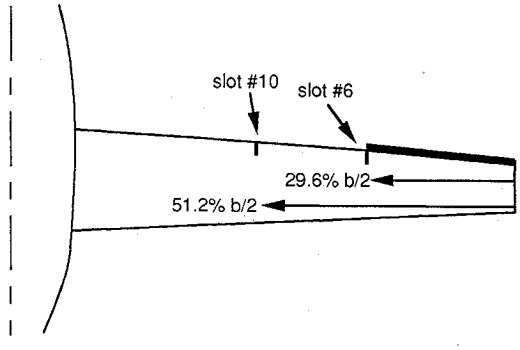

Fig. 9 Leading-edge droop/slots modification configuration.

Longitudinal Characteristics

Basic configuration characteristics. Presented in Fig. 11 are the lift and pitching moment characteristics of the basic model. These data indicate that a maximum lift coefficient C_L of 1.24 occurred at an angle of attack of $\alpha = 14$ deg. Between $\alpha = 14$ and 16 deg, C_L dropped sharply, indicating an abrupt stall. The pitching moment data, presented with the center of gravity at a location of 25% of the mean aerodynamic chord, show longitudinal stability throughout the angle-of-attack range tested. Pitch stability was reduced near the stall and was followed by a large nose-down pitch break.

Leading-edge modifications. Presented in Fig. 12 are the lift and pitching moment characteristics of the modified configuration compared to the basic model configuration. The lift curve shows a slight decrease in maximum lift coefficient with the wing modifications, but after the stall angle of attack, an increment in lift with the wing modifications makes the stall more gradual. The increment in lift was due to the increased amount of attached flow that the modifications provided. The pitching moment characteristics in Fig. 12 show that the modifications did not change the trim angle of attack or the longitudinal stability of the model.

Lateral-Directional Characteristics

The lateral-directional stability derivatives C_{l_β} and C_{n_β} were obtained from tests conducted at sideslip angles of +4 and −4 deg and are presented in Fig. 13 for the basic and modified configurations. The dihedral effect is indicated by the C_{l_β} vs α plot. For the basic configuration, C_{2_β} was negative from $\alpha = -8$ to 40 deg indicating a stable dihedral effect. From $\alpha = 12$ to 14 deg, C_{l_β} decreased abruptly. Since $\alpha = 14$ deg was the angle of attack at which the wing stalled, it was believed that this sudden change in C_{l_β} was due to an asymmetric stall. The model's directional stability is also shown in Fig. 13. This figure shows decreasing stability until, at $\alpha = 14$ deg, C_{n_β}

Table 1 Airfoil coordinates with leading-edge droop modifications at the tip station

Upper surface		Lower surface	
x/c	y/c	x/c	y/c
−0.0257	−0.0077	−0.0257	−0.0077
−0.0245	−0.0012	−0.0245	−0.0120
−0.0208	0.0056	−0.0208	−0.0161
−0.0147	0.0126	−0.0147	−0.0197
−0.0062	0.0198	−0.0062	−0.0230
0.0046	0.0269	0.0046	−0.0258
0.0177	0.0337	0.0177	−0.0282
0.0331	0.0402	0.0331	−0.0300
0.0506	0.0461	0.0506	−0.0315
0.0703	0.0513	0.0703	−0.0325
0.0919	0.0557	0.0919	−0.0331
0.1153	0.0594	0.1153	−0.0334
0.1500	0.0629	0.1405	−0.0336
0.2000	0.0655	0.1674	−0.0337
0.2025	0.0655	0.1958	−0.0337
0.2500	0.0661	0.2255	−0.0339
0.3000	0.0655	0.2564	−0.0342
0.3500	0.0639	0.3000	−0.0345
0.4000	0.0616	0.4500	−0.0343
0.4500	0.0586	0.5000	−0.0331
0.5000	0.0551	0.5500	−0.0313
0.5500	0.0512	0.6000	−0.0292
0.6000	0.0469	0.6500	−0.0267
0.6500	0.0422	0.7000	−0.0239
0.7000	0.0371	0.7500	−0.0208
0.7500	0.0318	0.8000	−0.0174
0.8000	0.0263	0.8500	−0.0138
0.8500	0.0204	0.9000	−0.0098
0.9000	0.0143	0.9500	−0.0056
0.9500	0.0078	1.0000	0.0000
1.0000	0.0000	—	—

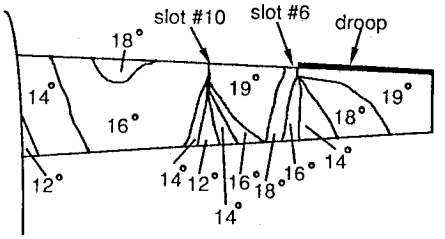

Fig. 10 Modified wing stall pattern (contour lines indicate areas of separated flow at the angle of attack shown).

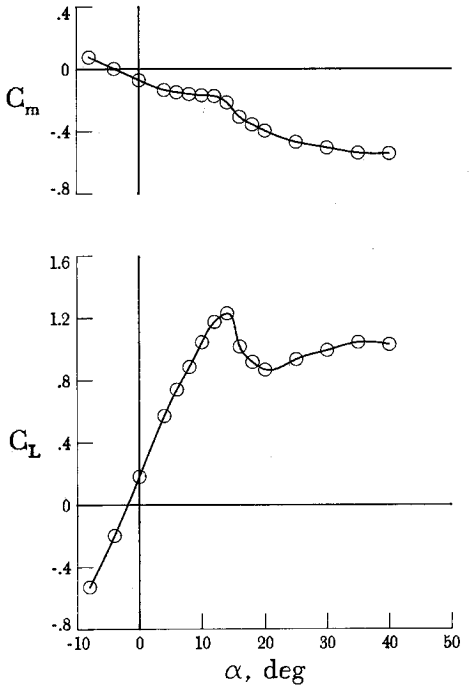

Fig. 11 Longitudinal characteristics of the basic configuration.

became unstable. Like C_{l_β} vs α, this sharp drop in C_{l_β} was probably caused by asymmetric stall. This asymmetry was caused by the uneven growth of stall cells, which could have been due to the model or to test conditions such as asymmetric leading edges, or crossflow in the wind tunnel.

The lateral-directional stability for the modified configuration, also shown in Fig. 13, indicates that the configuration also exhibited stable dihedral effect ($-C_{l_\beta}$). The effects of the leading-edge modifications on directional stability were primarily near stall. Similar to the baseline case, the directional stability curve shows a dip at stall due to asymmetric wing stall, which was less with the modifications.

Control Effectiveness

Figure 14 shows the lateral control effectiveness with aileron deflections of +5 and −5 deg on the left and right side flaperons, respectively, for the baseline configuration as compared to the modified configuration. It shows that, at high angles of attack, the droop/slot combination gave more aileron control. The modified wing had more attached flow over the control surface making it more effective. As expected with increasing angle of attack, the control power decreased as more of the flow separated.

Full-Scale Flight Tests

Flow Visualization Tests

The full-scale aircraft was not equipped to record data and so no quantitative data were collected; thus, pilot comments and observations made from inside the aircraft and from a chase plane during the tests were the primary sources of information. For stall testing, the aircraft was tufted with small pieces of yarn for flow visualization, and video and still photographs were made to record the flow patterns over the aircraft with the main emphasis being on the wing. Figure 15 shows a photograph taken from inside of the aircraft looking at the right wing with the droop/slot wing modification. The maneuver being performed at the time that the photograph was taken was a level flight idle power stall. The tuft pattern

Table 2 Airfoil coordinates with leading-edge droop modifications at the inboard station

	Upper surface	Lower surface
x/c	*y/c*	*y/c*
−0.0250	−0.0124	−0.0124
−0.0238	−0.0052	−0.0171
−0.0201	0.0023	−0.0215
−0.0140	0.0101	−0.0256
−0.0055	0.0182	−0.0292
0.0053	0.0264	−0.0324
0.0184	0.0345	−0.0351
0.0338	0.0425	−0.0373
0.0514	0.0500	−0.0391
0.0710	0.0568	−0.0403
0.0963	0.0637	−0.0412
0.1500	0.0719	−0.0423
0.2000	0.0751	−0.0429
0.2025	0.0751	−0.0430
0.2500	0.0760	−0.0437
0.3000	0.0755	−0.0446
0.3500	0.0739	−0.0448
0.4000	0.0713	−0.0445
0.4500	0.0680	−0.0437
0.5000	0.0640	−0.0419
0.5500	0.0595	−0.0396
0.6000	0.0545	−0.0368
0.6500	0.0491	−0.0336
0.7000	0.0433	−0.0300
0.7500	0.0371	−0.0261
0.8000	0.0307	−0.0218
0.8500	0.0238	−0.0172
0.9000	0.0167	−0.0123
0.9500	0.0092	−0.0070
1.0000	0.0000	0.0000

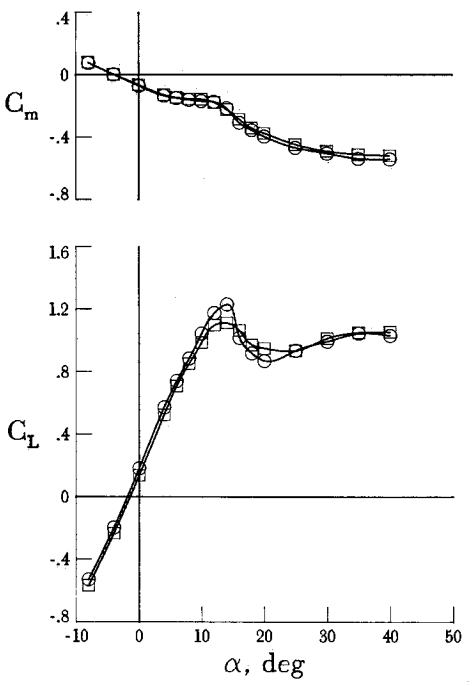

Fig. 12 Effect of the leading-edge modifications on the longitudinal characteristics.

shows attached flow on the outboard panel of the wing with some additional attached flow on the midpanel area and shows good agreement with the tuft pattern seen from the wind-tunnel tests (Fig. 10).

Longitudinal Characteristics

Basic configuration characteristics. According to the test pilot, the longitudinal stability of the basic, unmodified aircraft was excellent, a result in agreement with wind-tunnel data. The basic aircraft was not ever fully stalled during flight testing. It was only flown in an approach to a stall. Full stalls were not attempted because of the anticipated abrupt stall characteristics.

Leading-edge modifications. Longitudinal stability was unchanged with leading-edge modifications. This comment from flight test is in agreement with wind-tunnel data. The test

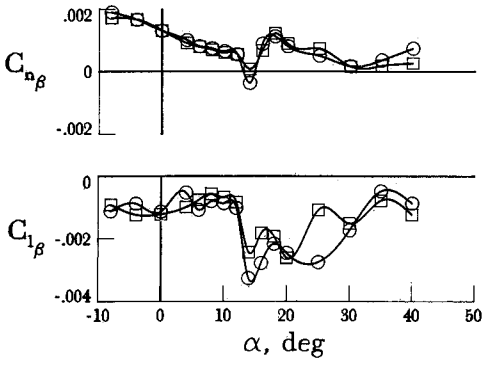

Fig. 13 Effect of the leading-edge modifications on the lateral-directional stability.

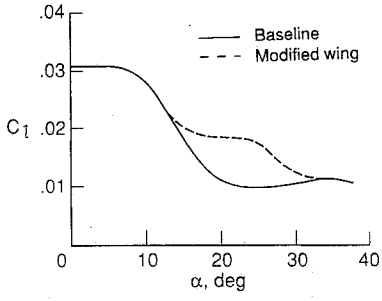

Fig. 14 Effect of the leading-edge modifications on the lateral control authority: $\delta_{a,\ \text{left}} = +5$ deg; $\delta_{a,\ \text{right}} = -5$ deg.

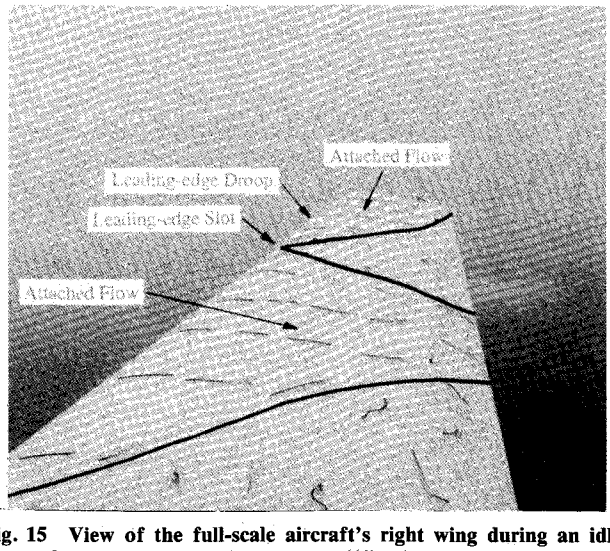

Fig. 15 View of the full-scale aircraft's right wing during an idle power, level stall with leading-edge modifications as seen from inside the cockpit.

pilot stated that the aircraft handled well in all cases and described the aircraft's handling through the stalls as pleasant. The level flight, power-off clean wing stalls generally demonstrated a right wing drop at approximately 72 knots of indicated airspeed (KIAS) and a gentle nose drop of about 5–10 deg at 68 KIAS. The wing drop was corrected easily with appropriate aileron deflection, and the airplane recovered immediately after the elevator deflection was relaxed. The level flight power-off stalls with flaps and landing gear extended showed results very similar to the clean wing stalls except that the wing drop normally occurred at 68 KIAS and the nose drop at 62 KIAS. The pilot added that this configuration sometimes caused a slight longitudinal oscillation that he called a porpoise action but stated that it was not of large amplitude and that it presented no control problems and ceased once the elevator deflection was relaxed. The pilot's comments for the power-on stalls were similar to the power-off stalls, except that the airplane's actions were quicker but still very controllable with no differences in controllability. The power-off clean wing stalls had a slight right wing drop at 69 KIAS and a nose drop at 65 KIAS. The power-on stalls with the flaps and landing gear extended did not exhibit the pitch oscillation that the power-off stall of the same type did, the wing drop did not occur until 65 KIAS, and the nose drop did not occur until 61 KIAS.

Lateral-Directional Characteristics

Basic configuration characteristics. Lateral-directional stability was good during all flight tests performed according to the test pilot. The wind-tunnel data showed slight directional instability at the stall angle of attack, but the instability was not detected in the full-scale tests when the aircraft was flown in an approach to the stall.

Leading-edge modifications. The change in lateral-directional stability of the aircraft due to the wing leading-edge modifications was unnoticeable or occurred in a flight regime that was not tested for the basic aircraft. This result was in agreement with the wind-tunnel results.

For the stalls tested with the leading-edge modifications on, the pilot reported that usually a right wing drop occurred. It was believed that this was caused due to some slight asymmetry between the incidence angles of the right and left wings. In approximately 5% of the tests, a slight directional oscillation occurred instead of the wing drop, but it was corrected easily with rudder. There were no uncontrollable lateral-directional motions throughout the maneuver, and the pilot stressed that he had lateral control of the airplane during the entire stall.

Control Effectiveness Characteristics

Basic configuration characteristics. The basic aircraft's elevator, flaperon, and rudder authority were very effective in controlling the aircraft. This information agreed with the wind-tunnel results, which predicted good control authority for all control surfaces. Flight tests have shown that the flaperons provided a roll rate of approximately 110 deg in the clean configuration at 150 KIAS.

Leading-edge modifications. With the leading-edge modifications on the aircraft, no change in control effectiveness was reported during normal flight. During stalls, all of the controls remained effective throughout the maneuvers and through recovery. When the wing drop occurred, flaperon authority was sufficient to level the wings, and when directional oscillations occurred, rudder deflection provided adequate control. Throughout the stall, the pilot had lateral control of the aircraft, which he demonstrated by performing right and left banking turns while maintaining full elevator deflection.

Conclusions

A wind-tunnel investigation was performed on a 22.5% scale model of a general aviation airplane to find a wing leading-edge modification that would improve the configuration's high angle-of-attack characteristics. The modification

found during these tests was then tested on a full-scale prototype aircraft. The major results of these tests can be summarized as follows.

1) The basic, unmodified configuration showed abrupt stall characteristics from flow visualization tests conducted in the wind tunnel. On the free-to-roll apparatus, the model exhibited large amplitude wing rock motion corresponding to the stalled flow conditions on the wing.

2) A wing leading-edge modification significantly improved the stall departure resistance. This modification was a combination of an outboard leading-edge droop with two chordwise leading-edge slots, one at the droop edge discontinuity and the other in the mid semispan region of the wing.

3) The modified configuration demonstrated minimal wing rock when tested on a free-to-roll apparatus.

4) Full-scale flight tests with the modified configuration demonstrated a gentle and easily controlled stall for all types of stalls tested, which included power-off and power-on stalls, entered with the wings level and in turning flight, all performed in both the clean wing configuration and with the flaps and landing gear extended.

5) From full-scale flight tests, lateral control was demonstrated throughout the entire stall maneuver for all types of stalls tested, which was demonstrated by the test pilot who performed left and right banking turns with the elevator fully deflected.

6) Qualitative analysis and flow visualization results indicated that a good general agreement between the wind-tunnel tests and full-scale flight tests was obtained.

Acknowledgments

The authors wish to thank Don Godwin, Jim Griswold, Doug Griswold, and Rich Gritter of Questair, Inc., for their support; D. M. Rao of Vigyan Research Associates, Inc., for development of the leading-edge slot concept for improved flow at high angles of attack; and Patrick King, U.S. Air Force, for development of a two-dimensional optimization technique for leading-edge droop design.

References

[1]Winkleman, A. E., and Barlow, J. B., "Flowfield Model for a Rectangular Planform Wing Beyond Stall," *AIAA Journal,* Vol. 18, No. 8, 1980, pp. 1006, 1007.

[2]Lan, C. T. E., and Roskam, J., *Airplane Aerodynamics and Performance,* Roskam Aviation and Engineering Corp., Ottawa, KS, 1981.

[3]Kroeger, R. A., and Feistal, T. W., "Reduction of Stall-Spin Entry Tendencies Through Wing Aerodynamic Design," Society of Automotive Engineers, Paper 760481, April 1976.

[4]Feistal, T. W., Anderson, S. B., and Kroeger, R. A., "A Method for Localizing Wing Flow Separation at Stall to Alleviate Spin Entry Tendencies," AIAA Paper 78-1476, Aug. 1978.

[5]Staff of NASA Langley Research Center, "Exploratory Study of the Effects of Wing Leading-Edge Modifications on the Stall/Spin Behavior of a Light General Aviation Airplane," NASA TP-1589, Dec. 1979.

[6]Johnson, J. L., Jr., Newsom, W. A., and Satran, D. R., "Full-Scale Wind Tunnel Investigation of the Effects of Wing Leading-Edge Modifications on High Angle-of-Attack Aerodynamic Characteristics of a Low-Wing General Aviation Airplane," AIAA Paper 80-1844, Aug. 1980.

[7]DiCarlo, D. J., Stough, H. P., III, and Patton, J. M., "Effect of Discontinuous Wing Leading-Edge Modifications on the Spinning Characteristics of a Low-Wing General Aviation Airplane," AIAA Paper 80-1843, Aug. 1980.

[8]Stough, H. P., III, DiCarlo, D. J., and Stewart, E. C., "Wing Modifications for Increased Spin Resistance," Society of Automotive Engineers, Paper 830720, April 1983.

[9]Murri, D. G., and Jordan, F. L., Jr., "Wind Tunnel Investigation of a Full-Scale General Aviation Airplane Equipped with an Advanced Natural Laminar Flow Wing," NASA TP-2772, Nov. 1987.

[10]Hahne, D., Jordan, F. L., Jr., Davis, P., and Muchmore, C. B., "Full-Scale Semi-Span Tests of an Advanced NLF Business Jet Wing," Society of Automotive Engineers, Paper 871860, Oct. 1987.

[11]Yip, L. P., King, P. M., Muchmore, C. B., and Davis, P., "Exploratory Wind Tunnel Investigations of the Low-Speed Stability and Control Characteristics of Advanced General Aviation Configurations," AIAA Paper 86-2596, Sept. 1986.

[12]Yip, L. P., Robelen, D. B., and Meyer, H. F., "Radio-Controlled Model Flight Tests of a Spin Resistant Trainer Configuration," AIAA Paper 88-2146, May 1988.